Derivation of the Impurity MPO for Single-Orbital Problems in Real Time

J.T.

(Dated: 4th June 2024)

Description of the method. We consider the single-impurity Anderson model, described by the Hamiltonian

$$H = \sum_{\substack{k \\ \sigma=\uparrow,\downarrow \\ \alpha=L,R}} \Big[\big(t_k d_\sigma^\dagger c_{k,\alpha,\sigma} + h.c.\big) + \epsilon_k c_{k,\alpha,\sigma}^\dagger c_{k,\alpha,\sigma} \Big] + H_{\rm imp}, \tag{1}$$

with $H_{\rm imp} = (\epsilon_d - U/2)\sum_\sigma \hat{d}_\sigma^\dagger \hat{d}_\sigma + U \hat{d}_\uparrow^\dagger \hat{d}_\uparrow \hat{d}_\downarrow^\dagger \hat{d}_\downarrow$. The impurity level described by fermions d_σ is coupled to two baths ($\alpha = L, R$) of free fermions $c_{k,\alpha,\sigma}$ with identical dispersion ϵ_k and tunnel couplings t_k, initially in thermal equilibrium (see top illustration in Fig. 1). Coulomb interaction $U \neq 0$ in $H_{\rm imp}$ gives rise to strong correlations in and out of equilibrium.

We are primarily interested in the real-time evolution of an impurity observable $\langle \hat{O}(t) \rangle$ starting from a factorized initial state $\rho(0) = \rho_L \otimes \rho_{\rm imp} \otimes \rho_R$, with $\rho_{L,R}$ equilibrium states at inverse temperatures $\beta_{L,R}$ and chemical potentials $\mu_{L,R}$. While conventional tensor-network approaches attempt to compactly represent $\rho(t)$, we instead express $\langle \hat{O}(t) \rangle$ as a Keldysh path integral over Grassmann trajectories of impurity and baths. Gaussian integration over the bath trajectories gives

$$\begin{aligned} \langle \hat{O}(t) \rangle \;\propto\; & \int \Big(\prod_{\sigma,\tau} d\bar{\eta}_{\sigma,\tau} d\eta_{\sigma,\tau} \Big) \mathcal{O}(\bar{\boldsymbol{\eta}}_t, \boldsymbol{\eta}_t) \\ & \times \exp\Big\{ \int_{\mathcal{C}} d\tau \Big[\sum_\sigma \bar{\eta}_{\sigma,\tau} \partial_\tau \eta_{\sigma,\tau} - i\mathcal{H}_{\rm imp}(\bar{\boldsymbol{\eta}}_\tau, \boldsymbol{\eta}_\tau) \Big] \Big\} \\ & \times \rho_{\rm imp}[\bar{\boldsymbol{\eta}}_0, \boldsymbol{\eta}_0] \prod_{\sigma=\uparrow,\downarrow} \exp\Big(\int_{\mathcal{C}} d\tau \int_{\mathcal{C}} d\tau' \bar{\eta}_{\sigma,\tau} \Delta(\tau,\tau') \eta_{\sigma,\tau'} \Big). \end{aligned} \tag{2}$$

Here $\bar{\boldsymbol{\eta}}_\tau = (\bar{\eta}_{\uparrow,\tau}, \bar{\eta}_{\downarrow,\tau})$ and $\boldsymbol{\eta}_\tau = (\eta_{\uparrow,\tau}, \eta_{\downarrow,\tau})$ parametrize the impurity trajectory. The IF is the last exponential in Eq. (2), defined by the hybridization function $\Delta(\tau,\tau') = \sum_\alpha \Delta^\alpha(\tau,\tau')$, where Δ^α fully encodes the dynamical influence of the bath α,

$$\Delta^\alpha(\tau,\tau') = \int \frac{d\omega}{2\pi} \Gamma(\omega) g^\alpha_{\tau,\tau'}(\omega). \tag{3}$$

The latter is determined by the bath's spectral density $\Gamma(\omega) = 2\pi \sum_k |t_k|^2 \delta(\omega - \epsilon_k)$ and non-interacting Green's function $g^\alpha_{\tau,\tau'}(\omega) = \big(n^\alpha_{\rm F}(\omega) - \Theta_{\mathcal{C}}(\tau,\tau')\big) e^{-i\omega(\tau-\tau')}$, where $n^\alpha_{\rm F}$ is the Fermi distribution at inverse temperature β_α and chemical potential μ_α and $\Theta_{\mathcal{C}}$ is the Heaviside step function on the Keldysh contour $\mathcal{C}$.

The difficulty in evaluating the path integral arises from the combination of non-Gaussianity (in $\mathcal{H}_{\rm imp}$) and time-non-locality (in $\Delta(\tau,\tau')$). The key idea of our method is to interpret Eq. (2) as a scalar product of fictitious states and operators defined in a fermionic Fock space on a temporal lattice. To that end, we note that the textbook expression in Eq. (2) is defined as the limit $M \to \infty$ of a discrete-time expression, obtained by dividing the full time evolution window $[0, T]$ into M steps of size $\delta t = T/M$; we fix a sufficiently large M. For our purpose, it is convenient to use a Trotter scheme that further splits the Trotter step into impurity and hybrization, leading to $8M$ trajectory variables per spin species along the discretized Keldysh contour, Fig. 2. We arrange these in two arrays, $\boldsymbol{\eta}_\sigma = (\eta_{\sigma,0^+}, \eta_{\sigma,0^-}, \ldots, \eta_{\sigma,(2M-1)^+}, \eta_{\sigma,(2M-1)^-})$ and analogously $\bar{\boldsymbol{\eta}}_\sigma$, with degrees of freedom alternating on the forward ($+$) and backward ($-$) branch of the Keldysh contour. A series of manipulations with the discrete-time path integral, including partial "particle-hole transformations" $\eta \leftrightarrow \bar{\eta}$, allows us to rewrite Eq. (2) in a scalar

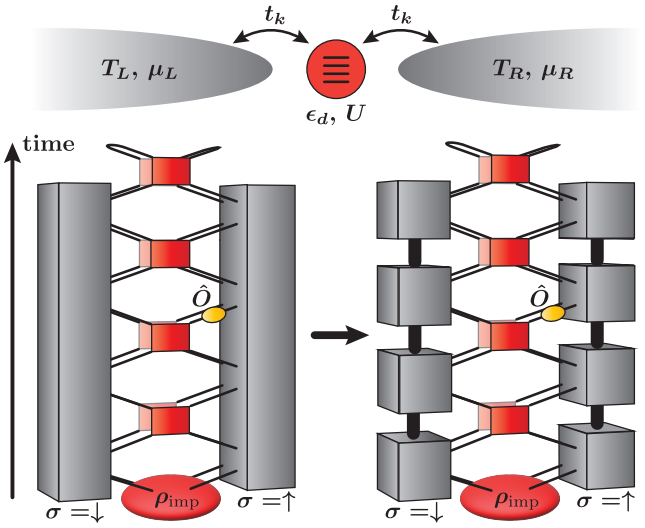

Figure 1. Top: Illustration of single impurity Anderson model [Eq. (1)] with an impurity (red) tunnel-coupled to two reservoirs (gray). Bottom: Tensor-network representation of a time-dependent observable $\langle \hat{O}(t) \rangle$. The dynamical influence of the environment is encoded in a single IF per orbital degree of freedom (here, two gray tensors for $\sigma = \uparrow, \downarrow$, left) which can be efficiently represented as MPS in the temporal domain (right) and hence contracted with the local impurity evolution (product of red tensors). Foreground [background] layer represents forward [backward] branch of the Keldysh contour.

product form (see Sec. I for details):

$$\langle \hat{O}(t) \rangle \propto \int \left(\prod_{\sigma} d\bar{\boldsymbol{\eta}}_\sigma d\boldsymbol{\eta}_\sigma \right) \times \mathcal{I}[\boldsymbol{\eta}_\downarrow] e^{-\bar{\boldsymbol{\eta}}_\downarrow \boldsymbol{\eta}_\downarrow} \mathcal{D}_{\mathcal{O},t}[\bar{\boldsymbol{\eta}}_\downarrow, \boldsymbol{\eta}_\uparrow]\, e^{-\bar{\boldsymbol{\eta}}_\uparrow \boldsymbol{\eta}_\uparrow} \mathcal{I}[\bar{\boldsymbol{\eta}}_\uparrow] \equiv \langle I | \hat{D}_{\hat{O},t} | I \rangle . \quad (4)$$

Here, the kernel $\mathcal{D}_{\mathcal{O},t}[\bar{\boldsymbol{\eta}}_\downarrow, \boldsymbol{\eta}_\uparrow]$, which is non-Gaussian, describes the impurity's own dynamics, and has a simple product form due to time locality. This gives rise to a product operator $\hat{D}_{\hat{O},t} = \hat{D}_1 \otimes \cdots \otimes \hat{D}_M$, where each $\hat{D}_m$ is a 16×16 matrix (except the first and last: see superimposed red tensors in Fig. 1) and $\hat{D}_{m^*=t/\delta t}$ contains $\hat{O}$. The discrete-time IF has a Gaussian form, $\mathcal{I}[\boldsymbol{\eta}_\sigma] = \exp\left(\boldsymbol{\eta}_\sigma^T \mathbf{B}\, \boldsymbol{\eta}_\sigma\right)$, where the antisymmetric matrix $\mathbf{B}$ is related to the time-discretization of $\Delta(\tau, \tau')$ (see SM). The Gaussian many-body wave function $|I\rangle$ associated with $\mathcal{I}$ (gray tensors in Fig. 1 bottom left) is obtained by replacing Grassmann variables by corresponding creation operators acting on the Fock space vacuum, $\boldsymbol{c}^\dagger \equiv (c^\dagger_{0^+}, c^\dagger_{0^-}, \ldots, c^\dagger_{(2M-1)^+}, c^\dagger_{(2M-1)^-})$,

$$|I\rangle = \exp\left(\mathbf{c}^{\dagger T} \mathbf{B}\, \mathbf{c}^\dagger \right) |\emptyset\rangle . \quad (5)$$

Such a state formally has a Bardeen-Cooper-Schrieffer form, regardless of the fermion-number conservation of the original problem, cf. Eq. (2); this is related to the "particle-hole transformations" performed to arrive at Eq. (4). We note that particle number conservation shows up as a sublattice symmetry in Eq. (5).

I. DERIVATION OF EQ. (4)

We start by recalling the standard derivation of the path integral in Eq. (2). Defining the evolution operator $U = \exp(i\,\delta t\, H)$ for a time step $\delta t = T/M$ ($M \gg 1$) and the Hamiltonian H from Eq. (1), the expectation value of an impurity observable can be expressed as

$$\langle \hat{O}(t_{m^*}) \rangle = \mathrm{Tr}_{\mathrm{imp}} \left[\mathrm{Tr}_{\mathrm{bath}} \left(U^{M-m^*}\, \hat{O}\, U^{m^*} \left(\rho_{\mathrm{imp}} \otimes \rho_{\mathrm{bath}}\right) (U^\dagger)^M \right) \right]. \quad (6)$$

Here, $t_{m^*} = m^* \cdot \delta t$ denotes a point on the discrete-time lattice and $m^* \in \{0, 1, \ldots, M\}$. This expression is cast into path integral form by inserting Grassmann resolutions of identity $\mathbb{1}_\tau = \otimes_\sigma \mathbb{1}_{\sigma,\tau}$, where

$$\mathbb{1}_{\sigma,\tau} = \int d(\bar{\eta}_{\sigma,\tau}, \eta_{\sigma,\tau}) d(\bar{\boldsymbol{\xi}}_{\sigma,\tau}, \boldsymbol{\xi}_{\sigma,\tau}) \; e^{-\bar{\eta}_{\sigma,\tau}\eta_{\sigma,\tau} - \bar{\boldsymbol{\xi}}_{\sigma,\tau}\boldsymbol{\xi}_{\sigma,\tau}} |\eta_{\sigma,\tau}, \boldsymbol{\xi}_{\sigma,\tau}\rangle\langle \bar{\eta}_{\sigma,\tau}, \bar{\boldsymbol{\xi}}_{\sigma,\tau}|, \quad (7)$$

between every multiplication of operators. Here, $\bar{\eta}_{\sigma,\tau}, \eta_{\sigma,\tau}$ are impurity variables with index

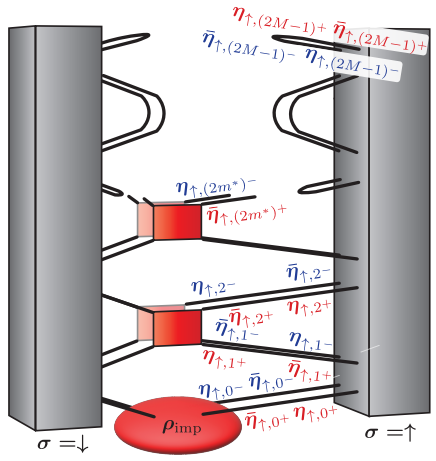

Figure 2. After inserting Grassmann resolutions of identity into Eq. (6), each leg of the IF and impurity tensor gets associated with a Grassmann variable [red (blue) color refers to the forward (backward) Keldysh branch]. Here, we show the density matrix of the impurity after two time steps. It is obtained from an IM containing $M = 4$ time steps. The impurity gates at time steps later than m^* are replaced by the identity operator.

$\tau = 0^\pm, \ldots, M^\pm$ on the (discretized) Keldysh contour, while $\bar{\boldsymbol{\xi}}_{\sigma,\tau} = (\bar{\xi}_{j=1,\sigma,\tau}, \ldots, \bar{\xi}_{j=L,\sigma,\tau})^T$, $\boldsymbol{\xi}_{\sigma,\tau} = (\xi_{j=1,\sigma,\tau}, \ldots, \xi_{j=L,\sigma,\tau})^T$ are the degrees of freedom of the environment (made of L fermionic modes). In total, we thus insert $2(M+1)$ identity resolutions per fermionic mode. In the limit $\delta t \to 0$, Eq. (2) is retrieved following standard textbook passages.

To define a clean prescription for our temporal wave functions overlap, however, it is more convenient to further split the evolution operator U into a local impurity and environment+tunneling evolution operators, i.e. $U \approx U_{\mathrm{imp}} \cdot U_{\mathrm{hyb}}$ (with the same error $\mathcal{O}(\delta t^2)$ as before). Here, we defined $U_{\mathrm{hyb}} = \exp\left(i\,\delta t\, H_{\mathrm{hyb}}\right)$ with

$$H_{\mathrm{hyb}} = H - H_{\mathrm{imp}} = \sum_{\substack{k \\ \sigma=\uparrow,\downarrow \\ \alpha=L,R}} \left[\left(t_k d^\dagger_\sigma c_{k,\alpha,\sigma} + h.c. \right) + \epsilon_k c^\dagger_{k,\alpha,\sigma} c_{k,\alpha,\sigma} \right], \quad (8)$$

and, for later convenience, we choose

$$U_{\mathrm{imp}} = \begin{cases} e^{i\,\delta t H_{\mathrm{imp}}} & \text{for evolution up to time } t_{m^*} \\ \mathbb{1}_{\mathrm{imp}} & \text{for evolution in range } [t_{m^*}, T]. \end{cases} \quad (9)$$

In total, with this modified Trotter decomposition, we insert $4M$ Grassmann identity resolutions per spatial site and $\tau = 0^\pm, \ldots, (2M-1)^\pm$. In Fig. 2, we illustrate how the resulting $8M$ Grassmann variables are associated with the legs of the IF and impurity tensors, respectively.

In order to arrive at the overlap form of Eq. (4), we manipulate the path integral in a way that results in

the following structure: All variables associated with the kernel of the spin-up (down) IF should be conjugate (non-conjugate) and opposite for the impurity kernel. This is achieved by making appropriate variable substitutions in the system-variables of the identity resolution, Eq. (7). We define these modified identity resolutions as

$$\mathbb{1}'_{\sigma,\tau} \quad \text{with substitution } \bar{\eta}_{\sigma,\tau} \to \eta_{\sigma,\tau},\ \eta_{\sigma,\tau} \to -\bar{\eta}_{\sigma,\tau}, \tag{10}$$

$$\mathbb{1}''_{\sigma,\tau} \quad \text{with substitution } \bar{\eta}_{\sigma,\tau} \to -\eta_{\sigma,\tau},\ \eta_{\sigma,\tau} \to \bar{\eta}_{\sigma,\tau}. \tag{11}$$

With this, Grassmann identities are inserted between the hybridization- and impurity evolution operators on the forward branch in the following way:

$$U_{\mathrm{imp}} \cdot \mathbb{1}_{(2m+1)^+} \cdot U_{\mathrm{hyb}} \cdot \mathbb{1}_{(2m)^+}, \tag{12}$$

with

$$\mathbb{1}_{(2m+1)^+} = \mathbb{1}_{\uparrow,(2m+1)^+} \otimes \mathbb{1}'_{\downarrow,(2m+1)^+}, \tag{13}$$

$$\mathbb{1}_{(2m)^+} = \mathbb{1}''_{\uparrow,(2m)^+} \otimes \mathbb{1}_{\downarrow,(2m)^+}. \tag{14}$$

On the backward branch, we insert identities as follows:

$$\mathbb{1}_{(2m)^-} \cdot U^\dagger_{\mathrm{hyb}} \cdot \mathbb{1}_{(2m+1)^-} U^\dagger_{\mathrm{imp}}, \tag{15}$$

with

$$\mathbb{1}_{(2m)^-} = \mathbb{1}_{\uparrow,(2m)^-} \otimes \mathbb{1}'_{\downarrow,(2m)^-}, \tag{16}$$

$$\mathbb{1}_{(2m+1)^-} = \mathbb{1}''_{\uparrow,(2m+1)^-} \otimes \mathbb{1}_{\downarrow,(2m+1)^-}. \tag{17}$$

With these insertions, one arrives at Eq. (4). Note that these variable substitutions alter the signs of some components of the impurity kernel, while they amount to a simple renaming of variables for the IF.

The resulting discrete-time IF has Gaussian form,

$$\mathcal{I}[\boldsymbol{\eta}_\sigma] = \exp\Big(\sum_{m,m'} \boldsymbol{\eta}^T_{\sigma,m} \mathbf{B}_{mm'} \boldsymbol{\eta}_{\sigma,m'} \Big), \tag{18}$$

with

$$\boldsymbol{\eta}_{\sigma,m} = (\eta_{\sigma,(2m)^+}, \eta_{\sigma,(2m)^-}, \eta_{\sigma,(2m+1)^+}, \eta_{\sigma,(2m+1)^-})^T.$$

The matrix $\mathbf{B}$ that appears here is the exact Gaussian influence action of the trotterized (Floquet) environment [53]. To understand its relation to the continuous-time result, it is convenient to express it in terms of a discrete-time hybridization matrix $\boldsymbol{\Delta}$,

$$\mathcal{I}[\boldsymbol{\eta}_\sigma] = \exp\left[\sum_{m \geq m'} \boldsymbol{\eta}^T_{\sigma,m} \boldsymbol{\Delta}_{mm'} \boldsymbol{\eta}_{\sigma,m} \right] e^{\eta_{\sigma,0^+}\eta_{\sigma,0^-}} \times e^{\sum_{m=0}^{M-1} \left(\eta_{\sigma,(2m+1)^+}\eta_{\sigma,(2m)^+} + \eta_{\sigma,(2m)^-}\eta_{\sigma,(2m+1)^-} \right)}, \tag{19}$$

where the terms in the second and third exponential in Eq. (19) stem from the overlap of Grassmann coherent states.

II. DETERMINING THE IMPURITY TENSOR

For an efficient numerical treatment, it is favorable to formulate the impurity operator $\hat{D}^{\hat{O}_1,\hat{O}_2}$ as product operator, such that it can subsequently be understood as matrix product operator with trivial bond dimension $\chi = 1$. Determining the sign in the individual tensors of $\hat{D}_{\hat{O}_t}$ is a nontrivial task as they depend on the global ordering of fermions along the Keldysh contour, fixed by the convention used for the IF. Here, we give a summary of this procedure.
Expanding the IF and impurity operator from Eq. (4) in full the many-body basis,

$$|I\rangle = \sum_\mu I_\mu |\mu\rangle \tag{20}$$

$$\hat{D}_{\hat{O}_t} = \sum_{\mu,\nu} |\nu\rangle \alpha_{\nu,\mu} \langle\mu|, \tag{21}$$

allows to associate each term with a specific impurity trajectory $|\mu\rangle$. With this, Eq. (4) can be expressed as,

$$\langle I|\, \hat{D}_{\hat{O}_t}\, |I\rangle \quad = \quad \sum_{\mu,\nu} I_\nu I_\mu \, \langle\nu| \Big(|\nu\rangle \alpha_{\nu,\mu} \, \langle\mu| \Big) |\mu\rangle, \tag{22}$$

where,

$$|\mu\rangle \equiv c^\dagger_i c^\dagger_j \dots c^\dagger_k |\emptyset\rangle, \tag{23}$$

$$\langle\mu| \equiv \langle\emptyset| c_k \dots c_j c_i, \qquad \Big(\text{note } \langle\mu| \neq |\mu\rangle^\dagger\Big), \tag{24}$$

$$|\nu\rangle \equiv c^\dagger_{k'} \dots c^\dagger_{j'} c^\dagger_{i'} |\emptyset\rangle, \tag{25}$$

$$\langle\nu| \equiv \langle\emptyset| c_{i'} c_{j'} \dots c_{k'}, \qquad \Big(\text{note } \langle\nu| \neq |\nu\rangle^\dagger\Big), \tag{26}$$

and $i < j < \dots < k$ with respect to a fixed ordering of variables along the Keldysh contour (and analogously $i' < j' < \dots < k'$). We fix the ordering to be,

$$\mathcal{C} \equiv \{\eta_{\uparrow,0^+}, \eta_{\uparrow,0^-}, \eta_{\uparrow,1/2^+}, \eta_{\uparrow,1/2^-}, \eta_{\uparrow,1^+}, \eta_{\uparrow,1^-}, \eta_{\uparrow,3/2^+}, \eta_{\uparrow,3/2^-}, \dots\} \tag{27}$$

and equivalently for the variables with $\sigma = \downarrow$.

Next, we describe how to derive the coefficients $\alpha_{\nu,\mu}$ for given local impurity gates which are fixed by U_{imp}, ρ_0^{imp}, and $\hat{O}_1$.

After making the appropriate variable substitutions in order to write the expectation value as overlap of wavefunctions, the Grassmann kernel $\mathcal{D}_{\hat{O}_t}$ can formally be factorized as follows:

$$
\begin{aligned}
&\mathcal{D}_{\hat{O}_t}[\{\bar{\eta}_{\downarrow,\tau},\eta_{\uparrow,\tau}\}]\\
=&\mathcal{D}_{M^*}[\bar{\eta}_{\downarrow,(2M-1)^+},\eta_{\uparrow,(2M-1)^-}]\\
&\cdot\mathcal{D}_{(M-1)^+}[\bar{\eta}_{\downarrow,(2M-3)^+},\bar{\eta}_{\downarrow,(2M-2)^+},\eta_{\uparrow,(2M-3)^+},\eta_{\uparrow,(2M-2)^+}]\\
&\cdot\cdot\mathcal{D}_{n^+}[\bar{\eta}_{\downarrow,(2n-1)^+},\bar{\eta}_{\downarrow,(2n)^+},\eta_{\uparrow,(2n-1)^+},\eta_{\uparrow,(2n)^+}]\dots\\
&\cdot\mathcal{D}_{0^*}[\bar{\eta}_{\downarrow,0^+},\bar{\eta}_{\downarrow,0^-},\eta_{\uparrow,0^+},\eta_{\uparrow,0^-}]\dots\\
&\cdot\mathcal{D}_{n^-}[\bar{\eta}_{\downarrow,(2n-1)^-},\bar{\eta}_{\downarrow,(2n)^-},\eta_{\uparrow,(2n-1)^-},\eta_{\uparrow,(2n)^-}]\dots\\
&\cdot\mathcal{D}_{(M-1)^-}[\bar{\eta}_{\downarrow,(2M-3)^-},\bar{\eta}_{\downarrow,(2M-2)^-},\eta_{\uparrow,(2M-3)^-},\eta_{\uparrow,(2M-2)^-}].
\end{aligned}
\tag{28}
$$

Here, the individual factors are the Grassmann kernels of the many-body operators from Eq. (6) and include the signs from the variable substitutions, Eqs. (10,11), e.g.

$$
\mathcal{D}_{n^+}=\langle\bar{\eta}_{\downarrow,(2n)^+},-\eta_{\uparrow,(2n)^+}|\hat{O}_tU_{\mathrm{imp}}|-\bar{\eta}_{\downarrow,(2n-1)^+},\eta_{\uparrow,(2n-1)^+}\rangle.
$$

It is clear that the polynomial that is obtained by multiplying out these kernels will lead to Grassmann strings that are not ordered according to Eq. (27). When bringing these into the correct order, each monomial picks up an individual sign if the number of necessary fermion swaps is odd.
Since it is favorable to avoid working with explicit many-body wavefunctions, we must include the signs *locally* in the kernels from Eq. (28).
For this, we proceed in the following way:

Step 1—We write each kernel $\mathcal{D}_m$ in terms of a matrix A_τ (containing weights $\alpha^\tau_{\nu,\mu}$ that correspond to local Grassmann strings at time τ) that defines a local map between the spin up and spin down many-body space at a given time step, e.g.:

$$
\mathcal{D}_{n^+}=\begin{pmatrix}1\\ \bar{\eta}_{\downarrow,(2n)^+}\\ \bar{\eta}_{\downarrow,(2n-1)^+}\\ \bar{\eta}_{\downarrow,(2n)^+}\bar{\eta}_{\downarrow,(2n-1)^+}\end{pmatrix}\boldsymbol{A}_{n^+}\begin{pmatrix}1\\ \eta_{\uparrow,(2n)^+}\\ \eta_{\uparrow,(2n-1)^+}\\ \eta_{\uparrow,(2n)^+}\eta_{\uparrow,(2n-1)^+}\end{pmatrix}.
\tag{29}
$$

We defined the basis such that each matrix element represents the weight $\alpha^n_{\nu,\mu}$ from Eq. (22) for a *local* string that is inversely ordered according to Eq. (27), separately for spin up and spin down. Note that the individual monomials in the basis vectors are arranged according to their binary representation in the ordering of Eq. (27).

Step 2— We swap the kernels in such a way that the kernels from the backward- and forward branch become interleaved, i.e. the new order is,

$$
\mathcal{D}_{\hat{O}_t}\to\mathcal{D}_{M^*}\mathcal{D}_{(M-1)^-}\mathcal{D}_{(M-1)^+}\dots\mathcal{D}_{n^-}\mathcal{D}_{n^+}\dots\mathcal{D}_{0^*}.
\tag{30}
$$

Importantly, this can give rise to a global minus sign in case two kernels with individually odd fermion parity are swapped. We determine the total number of global minus signs picked up in this way multiply the final result with the corresponding sign.

Step 3—Next, we perform manipulations on $\boldsymbol{A}_m$—i.e. on the *local* level—which ensure that the variables in the *global* impurity kernel $\mathcal{D}_{\hat{O}_t}$ are separated into spin up ($\eta_\uparrow$-variables) and spin down ($\eta_\downarrow$-variables).
To determine the necessary steps, it is convenient to go back to Eq. (30) and to note that the input- and output space ($\eta_{\uparrow,\tau}$ and $\bar{\eta}_\downarrow$ variables, respectively) are separated in each local kernel $\mathcal{D}_\tau$, see Eq. (29). We would like to establish this separation of variables also on the level of global Grassmann strings.

To this end, let's first consider an arbitrary monomial in $\mathcal{D}_{\hat{O}_t}$. As a first step towards separating variables in this monomial, we move the $\bar{\eta}_{\downarrow,(2M-2)^-}$ and $\bar{\eta}_{\downarrow,(2M-3)^-}$ variables contained $\mathcal{D}_{(M-1)^-}$ to the leftmost position, i.e. through the kernels $\mathcal{D}_{M^*}$.
Clearly, if there is an even number of spin down variables in $\mathcal{D}_{(M-1)^-}$, this operation does not change the sign of the monomial. If, on the contrary, there is an odd number of spin down variables, the sign of the string changes if the kernel $\mathcal{D}_{M^*}$ has odd parity. In that case, we multiply each term in $\boldsymbol{A}_{(M-1)^+}$ that corresponds to an odd number of spin down variables with a minus sign.

Next, we move each monomial of spin down variables from $\mathcal{D}_{(M-1)^+}$ to the leftmost position of the global Grassmann string. Analogously, if the Grassmann string to left of $\mathcal{D}_{(M-1)^+}$ has odd parity, we multiply coefficients that corresponds to an odd number of spin down variables in $\mathcal{D}_{(M-1)^+}$ with a minus sign.
Next, we move the spin down variables contained in $\mathcal{D}_{(M-2)^-}$, and update the signs in $\boldsymbol{A}_{(M-2)^-}$ and so on, until all spin down variables stand on the left of the spin up variables. At this stage, we have separated the input- and output variables and adjusted the signs of all weights in $\{\boldsymbol{A}_{m^\pm}\}$, such that they correspond to Grassmann strings in the ordering:

$$
\begin{aligned}
&\left(\bar{\eta}_{\downarrow,0^-}\bar{\eta}_{\downarrow,0^+}\right)\left(\bar{\eta}_{\downarrow,2^+}\bar{\eta}_{\downarrow,1^+}\right)\left(\bar{\eta}_{\downarrow,2^-}\bar{\eta}_{\downarrow,1^-}\right)\left(\bar{\eta}_{\downarrow,4^+}\bar{\eta}_{\downarrow,3^+}\right)\dots\\
&\times\left(\eta_{\uparrow,4^+}\eta_{\uparrow,3^+}\right)\left(\eta_{\uparrow,2^-}\eta_{\uparrow,1^-}\right)\left(\eta_{\uparrow,2^+}\eta_{\uparrow,1^+}\right)\left(\eta_{\uparrow,0^-}\eta_{\uparrow,0^+}\right),
\end{aligned}
\tag{31}
$$

where the first and second line correspond to the output- and input space, respectively.
While brackets of the spin up variables are already in the correct (descending) order according to Eq. (27), another step is necessary to reorder the output variables.

Step 4—Next, we bring the spin down variables into the same order as the spin up variables. For this, we proceed by first reversing the order in every pair of brackets. Let l denote the number of fermions inside a bracket. Then, reversing the Grassmann variables in these brackets introduces a minus sign if $\lfloor l/2\rfloor \pmod 2 = 1$, i.e. for $l=2,3,6,7,\dots$. We take this into account by adjusting

the signs in $\{\boldsymbol{A}_{m^\pm}\}$ for the corresponding entries. [Note that here, in the single-orbital case, $l \in \{0,1,2\}$.]
At this point, the spin down fermions are exactly in the opposite order from the spin up fermions. The last step must thus consist of globally reversing the string of output fermions. Note that the BCS structure of the IF imposes that the global string of spin down variables and the global string of spin up variables each have even parity. Reversing the string of $N_\downarrow$ spin down introduces a sign $(-1)^{N\downarrow/2} = (i)^{N\downarrow}$. We take this into account in the local kernels by including a factor of imaginary i for each spin down fermion in $\{\tilde{\boldsymbol{A}}_{m^\pm}\}$ which effectively counts the number of fermions and automatically produces a minus sign if $N_\downarrow/2 \pmod 2 = 1$ without the need to analyze the global string.

At this point, the variabels are in the order:

$$\Big(\bar\eta_{\downarrow,4^+}\bar\eta_{\downarrow,3^+}\Big)\Big(\bar\eta_{\downarrow,2^-}\bar\eta_{\downarrow,1^-}\Big)\Big(\bar\eta_{\downarrow,2^+}\bar\eta_{\downarrow,1^+}\Big)\Big(\bar\eta_{\downarrow,0^-}\bar\eta_{\downarrow,0^+}\Big)\dots \times \Big(\eta_{\uparrow,4^+}\eta_{\uparrow,3^+}\Big)\Big(\eta_{\uparrow,2^-}\eta_{\uparrow,1^-}\Big)\Big(\eta_{\uparrow,2^+}\eta_{\uparrow,1^+}\Big)\Big(\eta_{\uparrow,0^-}\eta_{\uparrow,0^+}\Big). \tag{32}$$

It remains to interleave the forward and backward variables that belong to a given time step.

Step 5— Locally, at a given point on the discrete time grid, the tensor product $\tilde{\boldsymbol{A}}_m \equiv \boldsymbol{A}_{m^+} \otimes \boldsymbol{A}_{m^-}$, contains the weights for local strings with variables $\eta_{\uparrow,\tau}$ and $\bar\eta_{\downarrow,\tau}$ mixed, but each of these two variable types is internally ordered as:

$$\{\eta_{\uparrow,(2m)^-}, \eta_{\uparrow,(2m-1)^-}, \eta_{\uparrow,(2m)^+}, \eta_{\uparrow,(2m-1)^+}\}, \tag{33}$$

and analogously for $\bar\eta_\downarrow$. We can thus work on the level of $\tilde{\boldsymbol{A}}_m$ to adjust the signs of each entry such that its components correspond to the weights of local "forward-backward-strings" ordered according to Eq. (27). To illustrate this procedure, let's the string,

$$\tilde{\boldsymbol{\alpha}}^m_{\nu,\mu}\,\bar\eta_{\downarrow,(2m-1)^-}\bar\eta_{\downarrow,(2m)^+}\bar\eta_{\downarrow,(2m-1)^+} \eta_{\uparrow,(2m)^-}\eta_{\uparrow,(2m-1)^-}\eta_{\uparrow,(2m)^+}\eta_{\uparrow,(2m-1)^+}, \tag{34}$$

weighted by the component $\tilde{\boldsymbol{\alpha}}_{\nu,\mu}$ that are contained in $\tilde{\boldsymbol{A}}_m$, for appropriate indices μ,ν. At this stage, we perform swaps between variables of the same type, to bring both variable types internally into the order of Eq. (27). These swaps will accumulate a minus signs. For the example in Eq. (34), it is easy to see that the string is equal to:

$$(-1)\times\tilde{\boldsymbol{\alpha}}^m_{\nu,\mu}\,\bar\eta_{\downarrow,(2m-1)^-}\bar\eta_{\downarrow,(2m)^+}\bar\eta_{\downarrow,(2m-1)^+} \eta_{\uparrow,(2m)^-}\eta_{\uparrow,(2m)^+}\eta_{\uparrow,(2m-1)^-}\eta_{\uparrow,(2m-1)^+}. \tag{35}$$

While this procedure is simple in the single-orbital case (where at most four variables need to be reordered), this step can be generalized for any string in more complicated models such that one obtains a procedure to adapt the signs in $\tilde{\boldsymbol{A}}_m$.

Crucially, a rearrangement of the basis elements is necessary, such that they are arranged in increasing order according to their binary representation w.r.t. the order from Eq. (27). With this, we obtain a sign-adjusted and reordered matrix, $\tilde{\boldsymbol{A}}_m$ which contains the correct weights $\tilde{\boldsymbol{\alpha}}^m_{\mu,\nu}$ for local "forward-backward-strings," where each variable type is internally ordered according to Eq. (27).